Dielectric function of sub-10 nanometer thick gold films

Ze Mei [1], Shuo Deng [1,2]*, Lijie Li [3], Xiaoyan Wen [1], Haifei Lv [1] and Min Li [1]*

[1] Department of Physics, Wuhan University of Technology, Wuhan 430070, China

[2] School of Electrical & Electronic Engineering, Nanyang Technological University, Singapore 639798, Singapore

[3] College of Engineering, Swansea University, Swansea SA1 8EN, UK

E-mail: dengshuo1990@whut.edu.cn & minli@whut.edu.cn

Abstract

A smooth gold (Au) film with thickness below 10 nanometers (*nm*) is hard to fabricate as well as to accurately measure its thickness and the corresponding dielectric function. Here, we report 5.4, 6.6 and 7.5 *nm* thick continuous Au films prepared on Chromium (Cr) seed layer. The thickness and dielectric function of the Au films are obtained using spectroscopic ellipsometry (SE) and first principles calculation. From the fitting results of the ellipsometric parameters, the value of the real part of dielectric function (ε_1) is negative almost in the whole spectrum region indicating that the Au films are continuous. For the imaginary part of dielectric function (ε_2), it decreases with increasing of the Au film thickness because the surface electrons scattering decreases. Moreover, the calculated and measured results of 5.4, 6.6 and 7.5 *nm* thick Au films present a good agreement in the wavelength range from 400 to 1600 *nm*. From the results of the first principles calculation, both ε_1 and ε_2 decrease with increasing of the Au film thickness. These precise measurement and calculation results of dielectric function are beneficial to nano-photoelectronic devices design with sub-10 *nm* Au films involved.

Keywords: Sub-10 *nm* thick Au film; Dielectric function; Spectroscopic ellipsometry; First principles calculation

Introduction

Gold (Au) has been one of the preferred materials for the application of the plasmonic and metamaterial because of its low optical loss, good chemical stability and high electrical conductivity [1-4]. It has been proved that the dielectric function of thin Au films is dependent on their thickness [5-8]. Hence, investigation the optical properties of Au films through dielectric function is an essential method for understanding the correlation between the device performances and characteristics of Au films. Although several studies have been reported on the dielectric function of Au films with different thicknesses recently, due to the poor wetting behavior of the Au film with the substrate

[9], most of the investigations focus on the Au films thicker than 10 *nm* [5-8]. Typically, in 2016, Hu *et al* measured the dielectric function of Au films in the thickness range from 8.5 to 44.3 *nm*, however one data (8.5 *nm*) in the thickness of sub-10 *nm* [5]. In 2017, Yakubovsky *et al* reported an experimental study for the dielectric function of Au films thickness between 20 and 200 *nm* [6]. Although the dielectric function for some continuous conductive Au films thickness between 3 and 9 *nm* are measured by spectroscopic ellipsometry (SE) in 2019, they mainly focused on the fabrication methods of Au films [7, 8]. To our best knowledge, no research on the dielectric function of sub-10 nanometers (*nm*) thick Au films based on both the SE and first principles calculation in detail. Moreover, the influences of film thickness on dielectric function in the sub-10 *nm* thick Au films is not clear yet.

In this paper, the dielectric function of 5.4, 6.6 and 7.5 *nm* thick Au films are investigated by the SE and the first principles calculation, which have been widely applied in prior research [10-11]. The first principles calculation results of dielectric function are consistent with the SE measurements. The calculated Au film thickness ceiling is 7.5 *nm* because the limitation of our computation ability. Due to our fabrication method cannot obtain a continuous structure when the Au film thickness is less than 5.4 *nm*, the first principles calculation investigates the dielectric function of 2.4, 3.3 and 4.2 *nm* thick Au films. Our results show that the values of the real (ε_1) and imaginary (ε_2) part of the dielectric function of the sub-10 *nm* thick Au films decrease with increasing of the Au film thickness. This work provides a reference for sub-10 *nm* thick Au film application in nano-photoelectric devices and as the absorber for the infrared light as well as metasurface.

Calculation Details and Fabrication Methods

All the calculations have been implemented by the first principles method with a free-standing Au film layer. A large vacuum spacing of 15 *Å* is added along the orthogonal direction of the Au (111) surface to avoid interaction of the periodic boundary conditions. The ion-electron interaction is described by the projector-augmented plane wave (PAW) potentials [12]. The exchange-correlation function of generalized gradient approximation (GGA) with the Perdew-Burke-Ernzerhof (PBE) [13] in the surface relaxation calculations is utilized. The *k*-points are $12\times12\times1$ and the mesh cutoff energy is 500 *eV*. The atomic structure is fully relaxed until the force on each atom becomes smaller than 0.01 *eV/Å* and the total energy change is smaller than 5×10^{-6} *eV*.

In our experiment, the Chromium (Cr) seed layer with identical thickness of 4 *nm* is firstly deposited by the

magnetron sputtering method with a 0.5 *mm* silicon substrate that has a 200 *nm* thick SiO_2 coating for various Au films. Then, the Au film is grown on the Cr seed layer as shown in Figure 1(a). Cr layer had been proved to be a suitable seed layer for the nanometer thick noble metals thin film fabrication in previous studies [14, 15]. In our magnetron sputtering progress, the main chamber is evacuated to a pressure below 3×10^{-4} *Pa* and a pure argon (Ar) gas working pressure of 2.0 *Pa* is used. The deposition rates are 0.67 *Å/s* for Cr and 0.89 *Å/s* for Au at room temperature. The variable-angle spectroscopic ellipsometry (J. A. Woollam VASE) is used to measure the thickness and dielectric function of Au films. Ellipsometric parameters (ψ, Δ) are acquired over the wavelength range from 400 to 1600 *nm* at three different incident angles for 65°, 70° and 75°, respectively. CompleteEASE software [16] is used to fit data between corresponding dielectric function and thickness.

Results and Discussion

The surface morphology of the Cr seeded Au film with the thickness of 5.4 *nm* is characterized by atom force microscope (AFM, Nanoscope IV) in the contact mode with the scanning area of $5\times5\ \mu m^2$. The AFM result is shown in Figure 1(b). It indicates that the surface roughness is uniform for all the measured areas with the root mean square (R_q) around 0.69 *nm*. This value demonstrates that the Au film surface of 5.4 *nm* thickness is smooth and favors for the SE measurements [17]. Figure 1(d) and 1(e) show the scanning electron microscope (SEM, Zeiss Ultra Plus) results of seeded and unseeded Au films with the thickness of 5.4 *nm*. From the SEM results, the continuity for seeded Au film (Figure 1(d)) is much better than unseeded one (Figure 1(e)). These results indicate that the high-quality sub-10 *nm* thick Au film can be fabricated on the Cr seed layer. The SEM results for the 4.2, 6.6 and 7.5 *nm* thick Au films are shown in Figure 1(f)-(h), respectively. Obviously, the 4.2 *nm* thick Au film is consisting of disconnect nano-island, while the others are continuous.

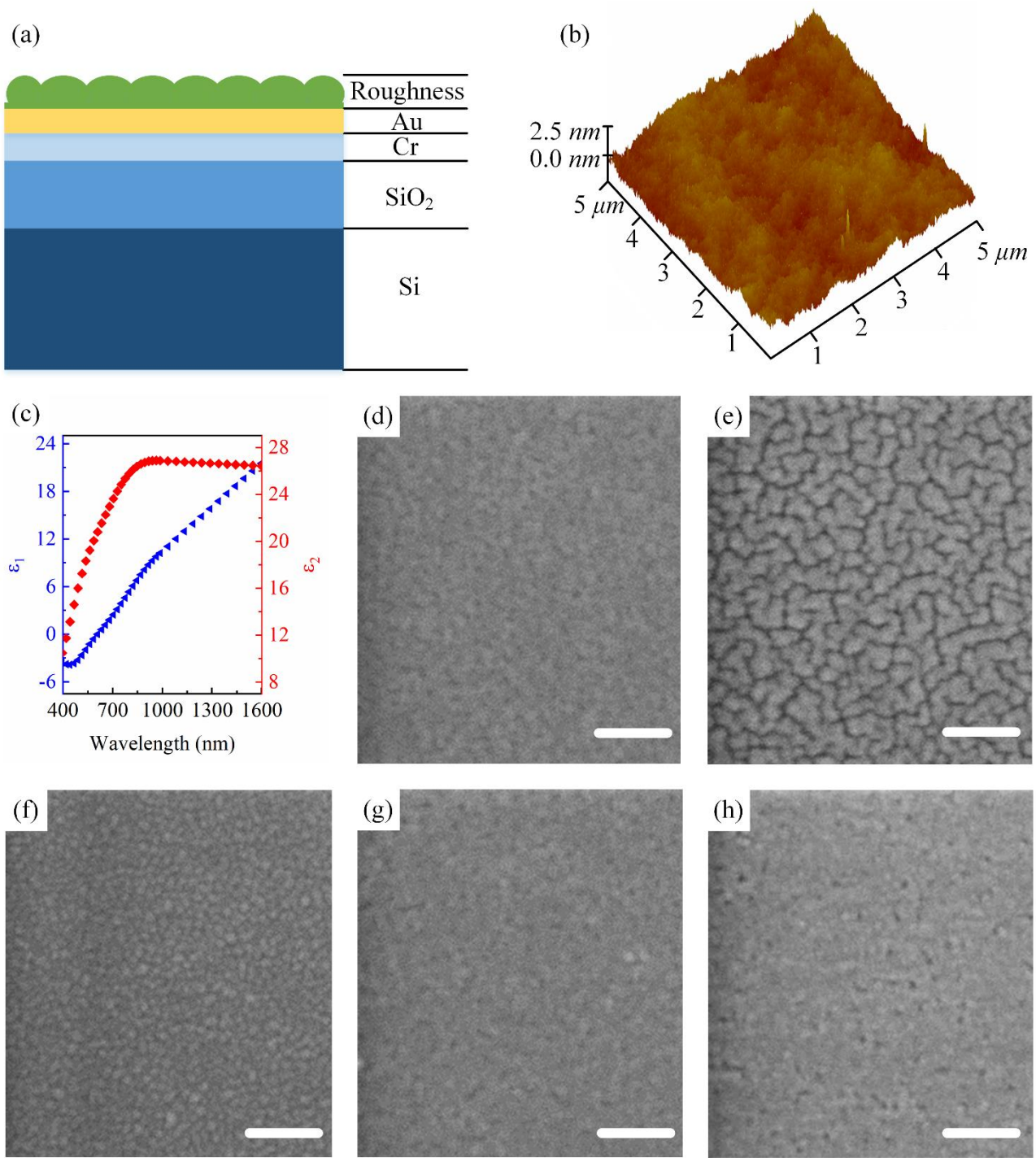

Figure 1: Schematic illustration of the roughness/Au/Cr/SiO_2/Si structure (a), AFM image for 5.4 *nm* thick Au film (b), the dielectric function of 4 *nm* thick Cr seed layer (c) and SEM images for seeded (d) and unseeded (e) Au films with the thickness of 5.4 *nm*. (f)-(h) show the SEM results of 4.2, 6.6 and 7.5 *nm* thick Au films, respectively. The scale bar in SEM results is 100 *nm*.

SE is used to measure the dielectric function of Au films with different thicknesses. The ellipsometric measurements

are described by the amplitude ratio (ψ) and the phase difference (Δ), which are defined by the amplitude reflection coefficients (ρ) of *p*- and *s*- polarizations [18]:

$$\rho = r_p / r_s = \tan(\psi)\exp(i\Delta) \tag{1}$$

where r_p and r_s are the amplitude reflection coefficients of the *p*- and *s*- polarized light, respectively. In order to obtain the thickness and dielectric function of the Au film, a five-layer optical model consisting of surface roughness layer/ Au layer/ Cr layer/ SiO_2 layer/ Si substrate is used in the fitting process as shown in Figure 1(a). The surface roughness layer can be depicted by the effective medium approximation (EMA) theory [19]. The Drude and critical points (DCP) [20] model is utilized to obtain the thickness and dielectric function of Au films, which can be expressed as:

$$\varepsilon(\omega) = \varepsilon_\infty - \frac{\omega_p^2}{\omega(\omega + i\Gamma_p)} + \frac{Ae^{i\varphi_1}}{\omega_1 - \omega - i\Gamma} + \frac{Ae^{-i\varphi_1}}{\omega_1 + \omega + i\Gamma} \tag{2}$$

where ε_∞ is the value of the high-frequency dielectric constant, which is assumed to be unity in all fitting processes. ω_p and Γ_p are the plasma frequency and Drude broadening, respectively. A, ω_1, φ_1 and Γ are the amplitude, energy, phase and broadening of the critical point, respectively. The optical properties of Cr/ SiO_2/ Si have been measured in advance to exclude the influence of dielectric function for Au films. The dielectric function of Cr seed layer is shown in Figure 1(c). The ε_1 and ε_2 of Cr seed layer increase with increasing of the wavelength. The difference between the fitting results and measurements is represented by the root mean square error (*RMSE*) [5]:

$$RMSE = \sqrt{\frac{1}{2n-m}\sum_{i=1}^{n}\left[\left(\frac{\psi_i^{\mathrm{mod}} - \psi_i^{\mathrm{exp}}}{\sigma_{\psi,i}^{\mathrm{exp}}}\right)^2 + \left(\frac{\Delta_i^{\mathrm{mod}} - \Delta_i^{\mathrm{exp}}}{\sigma_{\Delta,i}^{\mathrm{exp}}}\right)^2\right]} \tag{3}$$

where *n* is the number of the experimental points, *m* is the number of fitting parameters, σ is the standard deviation, $\psi_i^{\mathrm{mod}}\left(\Delta_i^{\mathrm{mod}}\right)$ and $\psi_i^{\mathrm{exp}}\left(\Delta_i^{\mathrm{exp}}\right)$ refer to the modeled and measured data, respectively.

The ellipsometric parameters for different Au film samples with error bars are shown in Figure 2. The error bars are very short because the error of phase difference and amplitude ratio are smaller than 0.02° and 0.07°, respectively. The fitting and measurement results present a good agreement in the entire measured spectral range of different thick Au films with the *RMSE* value of 0.42. It indicates that our fitting results are reliable and accurate in the

investigated spectrum range. The fitting parameters are given in Table 1. It can be found that the value of Drude damping factor $\left(\Gamma_p\right)$ decreases monotonically with increasing of the Au film thickness from 5.4 to 11.6 *nm* because the electrons scattering of imperfections and boundaries become less important as the Au film thickness increases. Moreover, the metallic behavior enhances with increasing of the Au film thickness. These results agree with the prior research [5, 21].

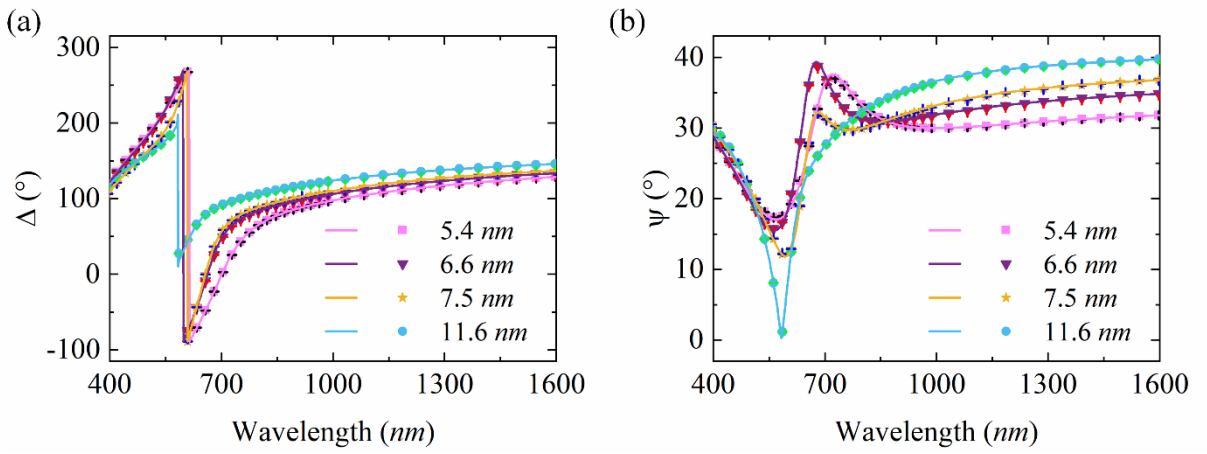

Figure 2: Measured (symbol) and fitting (line) ellipsometric parameters of phase difference $\left(\Delta\right)$ and amplitude ratio $\left(\psi\right)$ for the Au films with different thicknesses at 65° incident angle.

Table 1. Fitting parameters for different Au films thickness by using the DCP model.

thickness	5.4 *nm*	6.6 *nm*	7.5 *nm*	11.6 *nm*
RMSE	0.39	0.38	0.44	0.48
$\omega_p^2\left(eV^2\right)$	30.68 ± 0.44	31.64 ± 0.53	34.25 ± 1.13	41.12 ± 1.77
$\Gamma_p\left(eV\right)$	0.50 ± 0.01	0.48 ± 0.00	0.45 ± 0.01	0.39 ± 0.00
$A\left(eV\right)$	10.27 ± 0.04	9.52 ± 0.05	8.17 ± 0.08	7.48 ± 0.04
$\Gamma\left(eV\right)$	4.28 ± 0.06	1.90 ± 0.02	1.38 ± 0.01	1.08 ± 0.01
$\omega_1\left(eV\right)$	2.49 ± 0.03	2.72 ± 0.01	2.66 ± 0.00	2.80 ± 0.00
φ	-8.12 ± 0.41	-4.86 ± 0.39	-12.84 ± 0.13	4.11 ± 0.11

The dielectric function of Au films of different thickness with the data obtained from Johnson and Christy [22] are shown in Figure 3. With the increasing of the gold film thickness, our results are closing with the Johnson's data, which means our results are reliable. It shows that the ε_1 and ε_2 increase monotonically with decreasing of the film thickness. As shown in Figure 3(a), ε_1 is negative almost in the whole spectrum region for the film thickness investigated by us, indicating that the Au films are continuous [23]. Moreover, the value of ε_1 gets smaller with the increase of the Au film thickness because of the enhanced metallic behavior and the weakened electron-electron interaction [21]. This result is consistent with the variation of fitting parameter *A* in Table 1. In Figure 3(b), ε_2 decreases with increasing of the film thickness because the surface electrons scattering weakens, which further expands the Drude broadening $\left(\Gamma_p\right)$ [5].

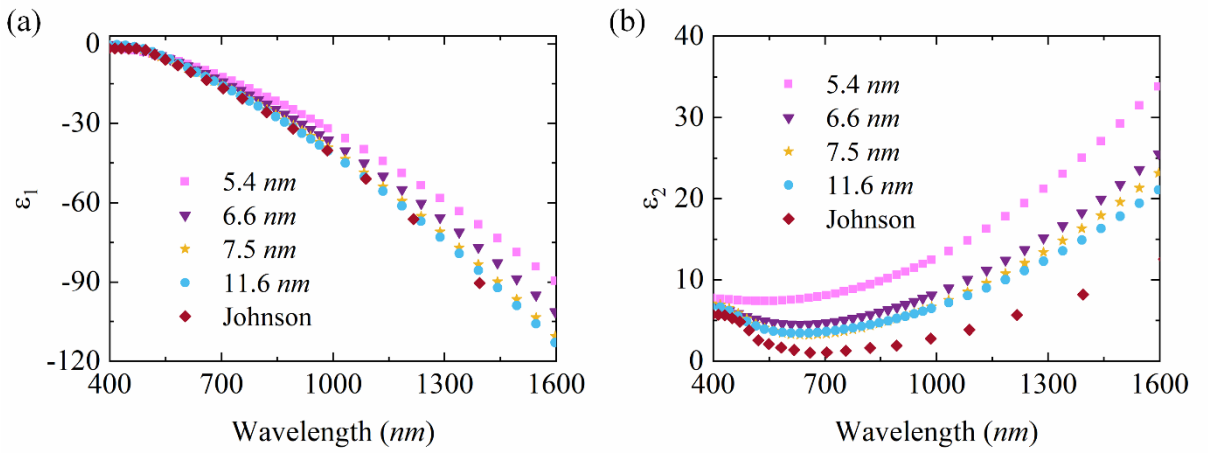

Figure 3: Real (a) and imaginary (b) part of the dielectric function for the Au films with different thickness.

Figure 4 shows the first principles calculation and SE measurement results of 5.4, 6.6 and 7.5 *nm* thick Au films, respectively. It can be observed a similar trend within the whole wavelength range for the first principles calculation and SE measurements. A deviation on the calculated and measured results of ε_2 can be observed, which is attributed to the fine-grained structure and the appearance of voids when the film thickness is in the sub-10 *nm* range. The difference between the first principles calculation and SE measurement results will weaken with increasing of the Au film thickness. Although a surface scattering can't be included in the first-principles calculation, a comparison to the experimental data is an important method for error estimate about the dielectric function results from first-principles calculation. Moreover, the prior work demonstrates that first-principles calculation is suitable for dielectric function investigation [11].

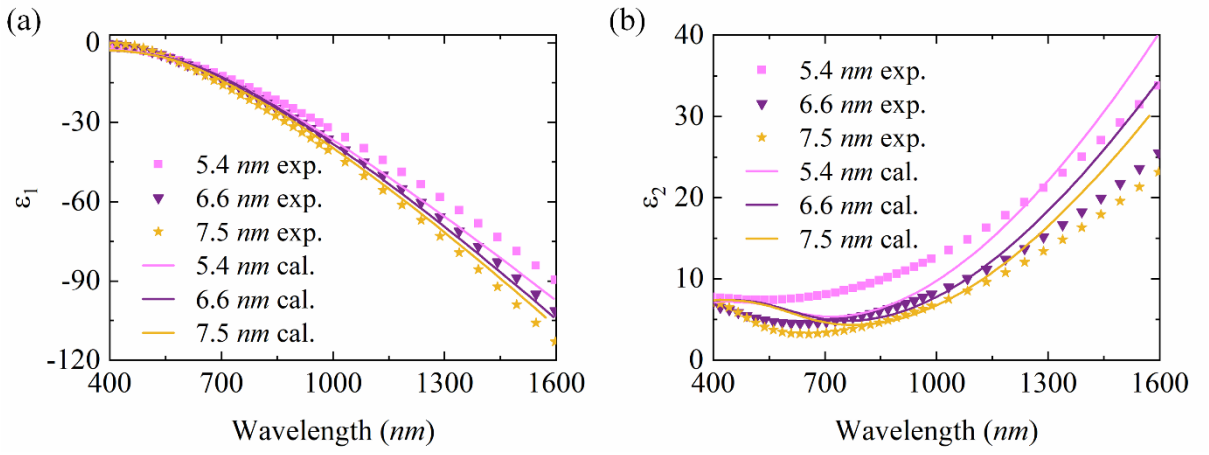

Figure 4: First principles calculation (line) and SE measurement (symbol) results of 5.4, 6.6 and 7.5 *nm* thick Au films, respectively.

Although getting the continuous Au film of sub-5 *nm* thick is very difficult by our fabrication method, the first principles calculation is a good way to investigate the dielectric function of sub-5 *nm* thick Au films. We extend the calculations for ε_1 and ε_2 of 4.2, 3.3 and 2.4 *nm* thick Au films. As shown in Figure 5, it is observed that the ε_1 remains negative in the whole spectral range and decreases with the wavelength increasing, which holds the similar trend to thicker films. Moreover, the ε_2 reaches a local maximum at the 450 *nm* wavelength and then increases linearly in the near-infrared range. The local maximum in ε_2 mainly arises from the electron interband transitions from the occupied states in the *d* band to the unoccupied states in the *sp* band [24]. The details of the density of states (DOS) results can be seen by the insert part of Figure 5(a). For comparison, the dielectric function of 3.63 *nm* Au film from reference [11] as shown in Figure 5, where the ε_1 ends at 1.7 *eV*. One can see a distinct difference in the dielectric function because the plasma frequency in our 3.3 *nm* thick Au film is 4.48 *eV*, which combines our prior spectroscopic ellipsometry measurement. However, the plasma frequency of 3.63 *nm* thick Au film (8.00 *eV*) in reference [11] only calculated from bulk structure.

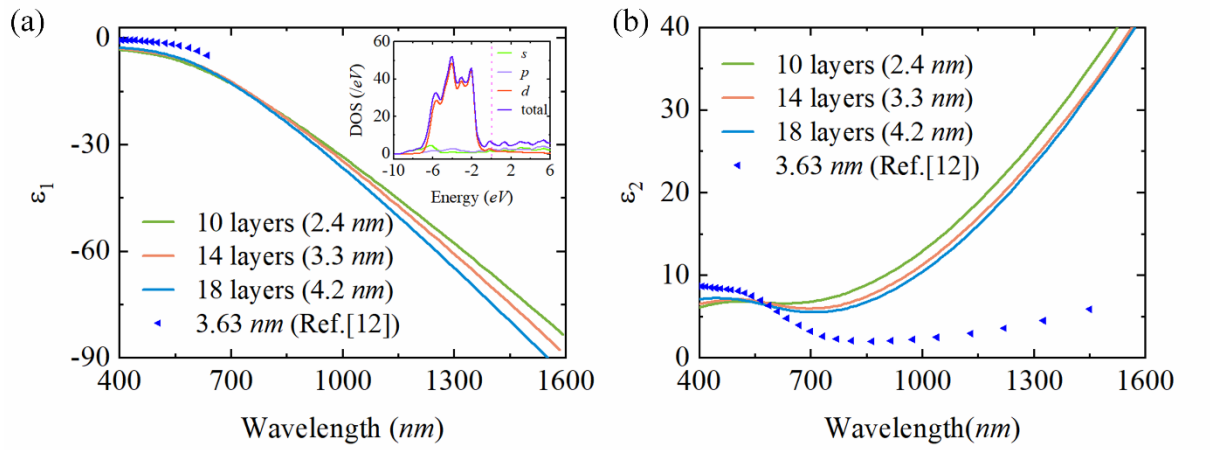

Figure 5: Real (a) and imaginary (b) part of the dielectric function for Au films thickness of sub-5 *nm* (inset showing the DOS results).

Conclusion

In summary, we have investigated the dielectric function of sub-10 *nm* thick Au films using the SE measurement and the first principles calculation. The SE measurement results are consistent with the first principles calculation for 5.4, 6.6 and 7.5 *nm* thick Au films. From the fitting results of the ellipsometric parameters, the ε_1 is negative almost in the whole spectrum region indicating that the Au films are continuous. For ε_2, it decreases with increasing

of the Au film thickness because the surface scattering of electrons enhances. From the first principles calculation results, both ε_1 and ε_2 decrease with increasing of the Au film thickness. These results will be helpful to explore the application of sub-10 *nm* thick Au films in nano-photoelectric devices.

Acknowledge

This work is supported by the National Natural Science Foundation of China (NSFC) (11974266, 62075174 and 11704293).

References

[1] Y. G. Bi, Y. F. Liu, X. L. Zhang, D. Yin, W. Q. Wang, J. Feng, and H. B. Sun, Adv. Opt. Mater. **7**(6), 1800778 (2019).

[2] J. Yun, Adv. Funct. Mater. **27**(18), 1606641 (2017).

[3] S. Link, P. Christopher, and D. B. Ingram, Nat. Mater. **10**(12), 911-921 (2011).

[4] J. Liu, H. He, D. Xiao, S. Yin, W. Ji, S. Jiang, D. Luo, B. Wang, and Y. Liu, Materials, **11**(10), 1833 (2018).

[5] E. T. Hu, Q. Y. Cai, R. J. Zhang, Y. F. Wei, W. C. Zhou, S. Y. Wang, Y. X. Zheng, W. Wei, and L. Y. Chen, Opt. Lett. **41**(21), 4907-4910 (2016).

[6] D. I. Yakubovsky, A. V. Arsenin, Y. V. Stebunov, D. Y. Fedyanin, and V. S. Volkov, Opt. Express **25**(21), 25574-25587 (2017).

[7] D. I. Yakubovsky, Y. V. Stebunov, R. V. Kirtaev, G. A. Ermolaev, M. S. Mironov, S. M. Novikov, A. V. Arsenin, and V. S. Volkov, Adv. Mater. Interfaces **6**(13), 1900196 (2019).

[8] R. A. Maniyara, D. Rodrigo, R. Yu, J. Canet-Ferrer, D. S. Ghosh, R. Yongsunthon, D. E. Baker, A. Rezikyan, F. J. García de Abajo, and V. Pruneri, Nat. Photonics **13**(5), 328-333 (2019).

[9] D. Dalacu, and L. Martinu, J. Opt. Soc. Am. B **18**(1), 85-92 (2001).

[10] H. U. Yang, J. D'Archangel, M. L. Sundheimer, E. Tucker, G. D. Boreman, and M. B. Raschke, Phys. Rev. B **91**(23), 235137 (2015).

[11] S. Laref, J. Cao, A. Asaduzzaman, K. Runge, P. Deymier, R. W. Ziolkowski, M. Miyawaki, and K. Muralidharan, Opt. Express **21**(10), 11827-18838 (2013).

[12] P. E. Blochl, Phys. Rev. B **50**(24), 17953-17979 (1994).

[13] J. P. Perdew, K. Burke, and M. Ernzerhof, Phys. Rev. Lett. **77**(18), 3865-3868 (1996).

[14] P. Melpignano, C. Cioarec, R. Clergereaux, N. Gherardi, C. Villeneuve, and L. Datas, Org. Electron. **11**(6), 1111-1119 (2010).

[15] S. D. Yambem, A. Haldar, K. S. Liao, E. P. Dillon, A. R. Barron, and S. A. Curran, Sol. Energy Mater. Sol. Cells **95**(8), 2424-2430 (2011).

[16] *CompleteEASE^{TM} Data Analysis Manual Version 4.63*, J. A. Woollam Co., Inc., Lincoln, NE, 2011, *pp*. 45.

[17] F. Zhang, R. J. Zhang, D. X. Zhang, Z. Y. Wang, J. P. Xu, Y. X. Zheng, L. Y. Chen, R. Z. Huang, Y. Sun, X. Chen, X. J. Meng, and N. Dai, Appl. Phys. Express **6**(12), 121101 (2013).

[18] H. Fujiwara, *Spectroscopic Ellipsometry: Principles and Applications* (John Wiley & Sons Ltd, Chichester, 2007), *pp*. 81.

[19] B. Fodor, P. Kozma, S. Burger, M. Fried, and P. Petrik, Thin Solid Films **617**(A), 20-24 (2016).

[20] P. G. Etchegoin, E. C. Le Ru, and M. Meyer, J. Chem. Phys. **125**(16), 164705 (2006).

[21] E. T. Hu, R. J. Zhang, Q. Y. Cai, Z. Y. Wang, J. P. Xu, Y. X. Zheng, S. Y. Wang, Y. F. Wei, R. Z. Huang, and L. Y. Chen, Appl. Phys. A-Mater. **120**(3), 875-879 (2015).

[22] P. B. Johnson, R. W. Christy, Phys. Rev. B **6**, 4370-4379 (1972).

[23] M. Hoevel, B. Gompf, and M. Dressel, Phys. Rev. B **81**(3), 035402 (2010).

[24] M. Xu, J. Y. Yang, S. Y. Zhang, and L. H. Liu, Phys. Rev. B **96**(11), 115154 (2017).